Supporting Information

Size-controlled and Shelf-stable DNA Particles for Production of Lentiviral Vectors

Yizong Hu[1,2,3,9], Yining Zhu[1,2,3,9], Nolan D. Sutherland[4], David R. Wilson[1,2,3], Marion Pang[1,3], Ester Liu[3,5], Jacob R. Staub[3], Cynthia A. Berlinicke[6], Donald J. Zack[6], Jordan J. Green[1,2,3,5,6,8], Sashank K. Reddy[7], and Hai-Quan Mao[1,2,3,8,*]

[1]Department of Biomedical Engineering, Johns Hopkins University School of Medicine, Baltimore, MD, USA. [2]Translational Tissue Engineering Center, Johns Hopkins University School of Medicine, Baltimore, MD, USA. [3]Institute for NanoBioTechnology, Johns Hopkins University, Baltimore, MD, USA. [4]bluebird bio, Inc., Cambridge, MA, USA. [5]Department of Chemical and Biomolecular Engineering, Johns Hopkins University, Baltimore, MD, USA. [6]Department of Ophthalmology, Johns Hopkins University School of Medicine, Baltimore, MD, USA. [7]Department of Plastic and Reconstructive Surgery, Johns Hopkins University School of Medicine, Baltimore, MD, USA. [8]Department of Materials Science and Engineering, Johns Hopkins University, Baltimore, MD, USA. [9]These authors contributed equally: Yizong Hu and Yining Zhu. *e-mail: hmao@jhu.edu.

List of Content

METHODS

Cell cultures and transfection studies. For monolayer culture studies, HEK293T cells (American Type Culture Collection, USA; maintained in DMEM + 10% FBS and 2 mM L-glutamine, at 37 °C, 5% CO_2, and saturated humidity) were seeded into 24-well plates at a cell density of 25,000 cells well^{-1} 1 day prior to transfection. The particles were pipetted into FreeStyle 293 medium in 5-ml microcentrifuge tubes, immediately followed by vortex for 10 sec to reach a final particle concentration of 1 μg pDNA ml^{-1}. For example, 100 μl of a particle suspension at 25 μg pDNA ml^{-1} was pipetted into 2.4 ml of serum-free FreeStyle 293 medium. The original medium in the wells was then drained and replaced by 500 μl of the particle-containing medium. At 4 h post-dosing, the medium was replaced by fresh full medium. A 20-h incubation was followed to allow transgene expression. For suspension culture studies, HEK293F cells (Thermo Fisher Scientific, USA; maintained in FreeStyle 293 medium, at 37 °C, 8% CO_2, and saturated humidity) were seeded into a 12-well plate equipped with a SpinΩ^{TM} Bioreactors plate spinner (3Dnamics, USA) at a cell density of 0.5 × 10^6 cells ml^{-1} at 1 day prior to transfection. The spinner was motorized at a rate of 150 rounds per minute for the duration of the experiments. The particles were pipetted into the wells all at once, followed by brief shaking of the plate, giving a final particle concentration of 1 μg pDNA ml^{-1}. For example, 80 μl of a particle suspension at 25 μg pDNA ml^{-1} was pipetted into 2 ml of the cell suspension within a single well. When a whole plate was finished, the spinner was reconnected. A 48-h incubation was followed to reach the peak transgene expression. When characterizing luciferase as the reporter, the cells were lysed by reporter lysis buffer (Promega, USA) using two freeze-thaw cycles, with the lysate characterized by a luminometer upon addition of luciferin assay solution (Promega, USA) against a ladder generated by the standardized luciferase samples (Promega, USA). When characterizing GFP as the reporter, the cells were suspended by trypsin-EDTA in PBS supplemented with 1% FBS and 0.5 mM EDTA and analyzed by a FACSCanto flow cytometer (BD Life Sciences, USA).

Assembly of stable particles at different sizes. The pDNA/PEI nanoparticles as the building blocks were first synthesized based on our previous reports.[1, 2] Briefly, pDNAs (multiple species with gWiz-Luc or gWiz-GFP from Aldevron, USA as a reporter) and PEIpro (Polyplus, France) were separately dissolved in ultrapure water, then pumped into a confined impinging jet (CIJ) mixer[3, 4] at a flow rate of 20 ml min^{-1}. The concentration was either 100 μg pDNA ml^{-1} (**Fig. 2**, generating 60 to 70-nm nanoparticles) or 200 μg pDNA ml^{-1} (**Fig. 5,** generating 80 to 100-nm nanoparticles); and the N/P ratio was 5.5. For small-batch preparations (**Fig. 2–4**), 100 μl of PBS solution (from 0.2× to 2×) was pipetted into 100 μl of the 60-nm nanoparticle suspension, immediately followed by 3 sec of vortex. At different time points (shown in **Fig. 2b**), 200 μl of the 20 mM HCl in 19% (w/w) trehalose solution was pipetted into the growing particles, immediately followed by 3 sec of vortex. The particles were stabilized and ready for use and characterization. For large-scale productions of the pDNA/PEI particles (**Fig. 5**), the 80 to 100-nm

nanoparticles and PBS (0.4× or 0.45×) were loaded in syringes separately and pumped into a CIJ device at a flow rate of 20 ml min^{-1}. The elute was collected and incubated under room temperature without stirring. When particles reached the target size, the particle suspension, and the solution of 2.5 mM HCl in 19% (w/w) trehalose were loaded in syringes separately and pumped into the CIJ device at a flow rate of 20 ml min^{-1}. The particles were ready for use or freezing down to -80 °C for long-term storage. In brief, For transfection experiments, the frozen particles were retrieved by thawing at ambient temperature followed by a brief vortex. The particles were then ready for use or temporarily stored for up to 1–2 days at ambient temperature without compromising transfection activity.

Dynamic light scattering (Zetasizer ZS90, Malvern, USA) was conducted periodically to monitor the size. A UV absorbance method using spectrophotometer (Nanodrop 1000, Thermo Fisher Scientific, USA) was used to assess the DNA concentration in particle suspensions. In brief, DNA molecules in a complexed form with PEI still yield linear correlations between the concentration and the absorbance at 260 nm, though with a reduced extinction coefficient compared with the uncomplexed free DNA (*cf.* Figure S4 in our previous publication[2]). A standard curve was first generated with stable pDNA/PEI nanoparticles at known concentrations, and the absorbance of the samples at 260 nm was measured with the pDNA concentration then calculated using the standard curve. This was used to monitor pDNA preservation and concentration change as reported in main text (**Fig. 2g, 5c**, and **d)**.

Quantitative cellular uptake and endosomal escape assessments by Cellomics. pDNA was labeled by covalently linking Cy5-amine (Lumiprobe, USA) to pDNA *via* UV-induced crosslinking of NHS-psoralen (Thermo Fisher Scientific, USA).[5] The Cy5-labeled pDNA was blended into the pDNA mixture at 5% prior to particle formulation. B16F10 cell line expressing GFP-coupled galectin-8 (GFP-Gal8) was obtained by transfection using plasmids encoding Super PiggyBac Transposase (System Biosciences, USA) and Piggybac-transposon-GFP-Gal8 (Addgene plasmid #127191) and a poly(beta-amino ester) (PBAE) carrier,[6] then sorted by a SH800 cell sorter (Sony, Japan) twice. The cells were cultured in DMEM supplemented with 10% FBS at 100,000 cells per well. The particles were dosed 24 h later as described above, except the transfection medium was switched to Opti-MEM for optimal results in this cell line. After incubation of predetermined times, cells were washed by PBS for three times, fixed by 4% paraformaldehyde (PFA) solution, stained by Hoechst 33342, and then washed by PBS for three times.

The plates were analyzed by a CellInsight CX7 High-content Analysis (HCA) platform (Thermo Fisher Scientific, USA). A brief example of the analysis process is given in **Fig. 4a**. Imaging was conducted at 20× magnification with a resolution of 1104 × 1104 $pixel^2$ per field correlating with an area of 501.2 × 501.2 μm^2. A total of 30 fields were analyzed inside each well of the plates, and the well-averaged result was generated by averaging all the cells in all the fields. The <SpotDetector.V4> program was used as supplied by the manufacturer with laser/filter sets of Channel 1: 386/440 nm, Channel 2: 485/521 nm, and Channel 3: 650/694 nm with fixed exposure times. In the analysis, the identifications of cell nuclei, GFP-Gal8 spots and

Cy5-pDNA spots were carried out with appropriate smoothing and thresholding settings that were verified by eye to obtain correct recognitions in sample images. In thresholding, <Isodata> (comparing each pixel with its surrounding) was used for GFP-Gal8 due to its high background (cytosolic Gal8); while <Fixed> (setting a predetermined level) was used for Cy5-pDNA due to its clean background, potentially irregular shapes, and large areas. Cell body (cytosolic area) identification and segmentation were approximated by extending the area attributed from each identified nucleus outward by 30 pixels (13.6 μm) with no overlap between adjacent cells (**Fig. 4a**).

Production of LVVs on ambr® 15 micro-bioreactor. Particles at different sizes were produced in the Mao Laboratory, stored at -80 °C and shipped on dry ice to bluebird bio, Inc., where the particles were stored under -80 °C until use. In-house suspension adapted HEK293T cells were seeded into 15 ml ambr® 15 micro-bioreactors (Sartorius Stedim Biotech, France). When cells reached a predetermined density, the cultures were perfused one vessel volume, then transfected with particles at an equivalent DNA concentration of 1 or 2 μg ml^{-1} by addition of corresponding volumes of the thawed particles at 50 μg pDNA ml^{-1} using the automated pipetting of the liquid handler. Parallel manually mixed pDNA/PEI particle transfections were performed using the same process conditions. After a predetermined incubation time, the micro-bioreactors were perfused one vessel volume again. The microbioreactor cultures were harvested and clarified by centrifugation at 500 $\times g$ for 5 min. The supernatants were sampled for analysis. Infectious titer results in titer units per ml (TU ml^{-1}) were determined by qPCR and the capsid protein p24 (ng ml^{-1}) was assessed by an enzyme-linked immunosorbent assay (Alliance HIV-I p24 ELISA Plate Kit, Perkin Elmer, USA). The p24 value was an indicator of total LVV particles, and the ratio between infectious titer and p24 detected was derived to particle-to-infectivity (P:I) ratio. For example, a P:I of 100 means that there is one functional LVV out of 100 viral particles produced.

Production of LVVs at the bench-scale. The same suspension adapted HEK293T cell line was used and seeded into an in-house developed 2-l single-use bioreactor. When cells reached a predetermined density, the cultures were perfused with one vessel volume utilizing an alternating tangential flow device, then transfected with particles at an equivalent DNA concentration of 1 or 1.5 μg ml^{-1} by addition of corresponding volumes of the thawed particles at 50 μg pDNA ml^{-1} using a peristaltic pump. The cultures were then harvested at the peak expression and clarified by depth filtration. Purification of the LVVs was then completed utilizing a standard resin-based chromatography followed by ultrafiltration and diafiltration into the final formulation. Infectious titer and p24 results were then determined using the described methods above.

SUPPLEMENTARY FIGURES

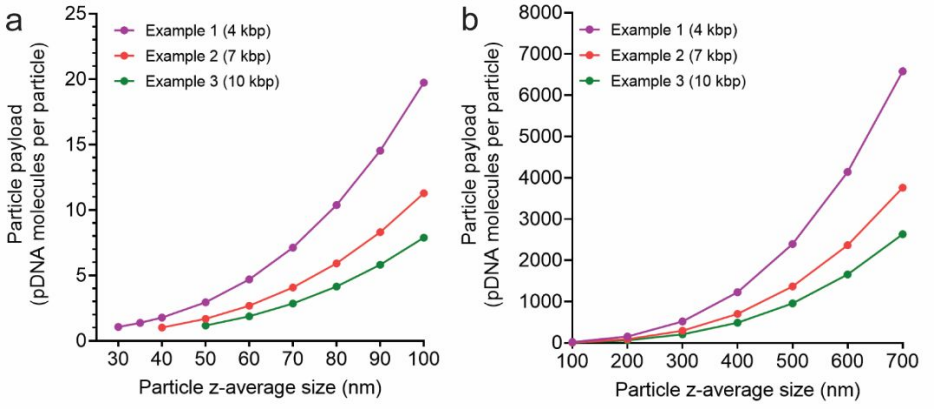

Supplementary Figure S1. The correlation of pDNA payload with size of pDNA/PEI particles. The theoretical pDNA payload (number of pDNA copies) per pDNA/PEI particle is shown when assuming the length of the pDNA is 4, 7 or 10 kbp, in the size range of **a,** 30 to 100 nm; or **b,** 100 to 700 nm.

Additional Notes on Supplementary Figure S1:

Our previous paper[2] on the kinetics of the assembly of pDNA/PEI particles suggested that the weight-average molar mass of the particles is linearly proportional to the z-average particle diameter to the third power, regardless of the mixing condition. The results across different N/P ratios were also similar.

$$[M_w, \mathrm{Da}] = 67.7 \times [D_Z, \mathrm{nm}]^3 + 1.9 \times 10^6$$

The rough calculations adopt 650 Da per bp for double-stranded pDNA, a constant bound PEI fraction[2, 7] that is equivalent to N/P = 2.7 to 3.0, and a molecular weight of one repeat unit of linear PEI as 43 Da. Therefore, the total molar mass of a single pDNA with all its associated PEI can be determined to be around 880 Da per bp. The correlation of theoretical pDNA payload per pDNA/PEI particle and particle size can then be derived from the above equation. Considering common pDNAs bearing a functional expression cascade have a length range of 4 to 10 kbp, three examples of pDNA with a length of 4, 7 or 10 kbp are shown in **Supplementary Fig. 1a,b** to demonstrate the payload-size correlation. Notably, a 400 to 500-nm particle contains roughly 1000 to 2500 pDNAs for 4 kbp pDNA, and 500 to 1000 pDNAs for 10 kbp pDNA, which are too high to assemble in a single step within the short particle assembly time.

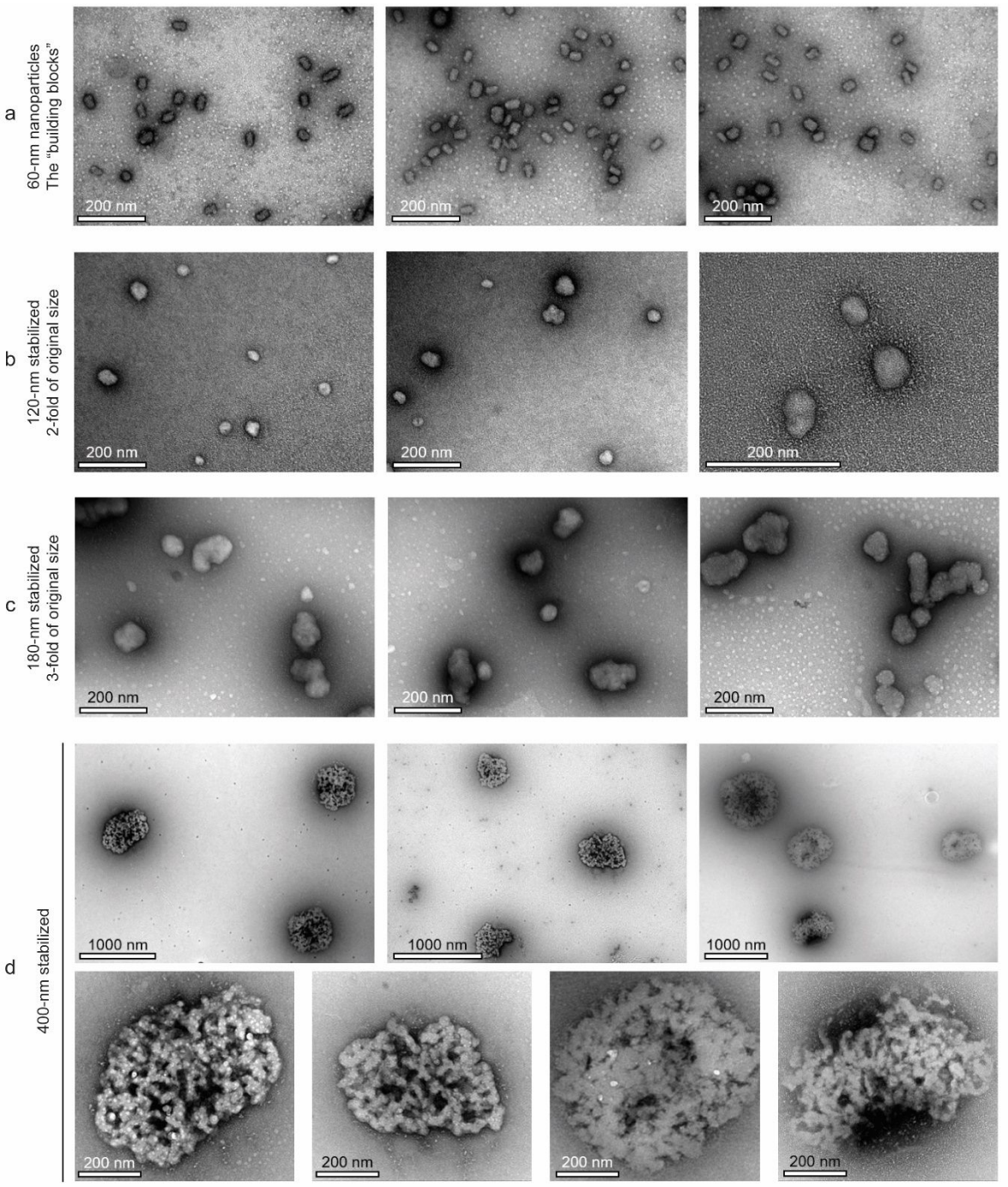

Supplementary Figure S2. Transmission electron microscopy (TEM) images of particles at the original or stabilized grown sizes. a, Images of the building block, 60-nm nanoparticles, produced by the flash nanocomplexation method[3]. In a size growth process, the particles were stabilized at **b,** double (120 nm) or **c,** triple (180 nm) of the original size to show the growth mechanism of association at interfaces upon contact of individual 60-nm nanoparticles. **d,** Populational features of stabilized 400-nm particles among different fields of the TEM images.

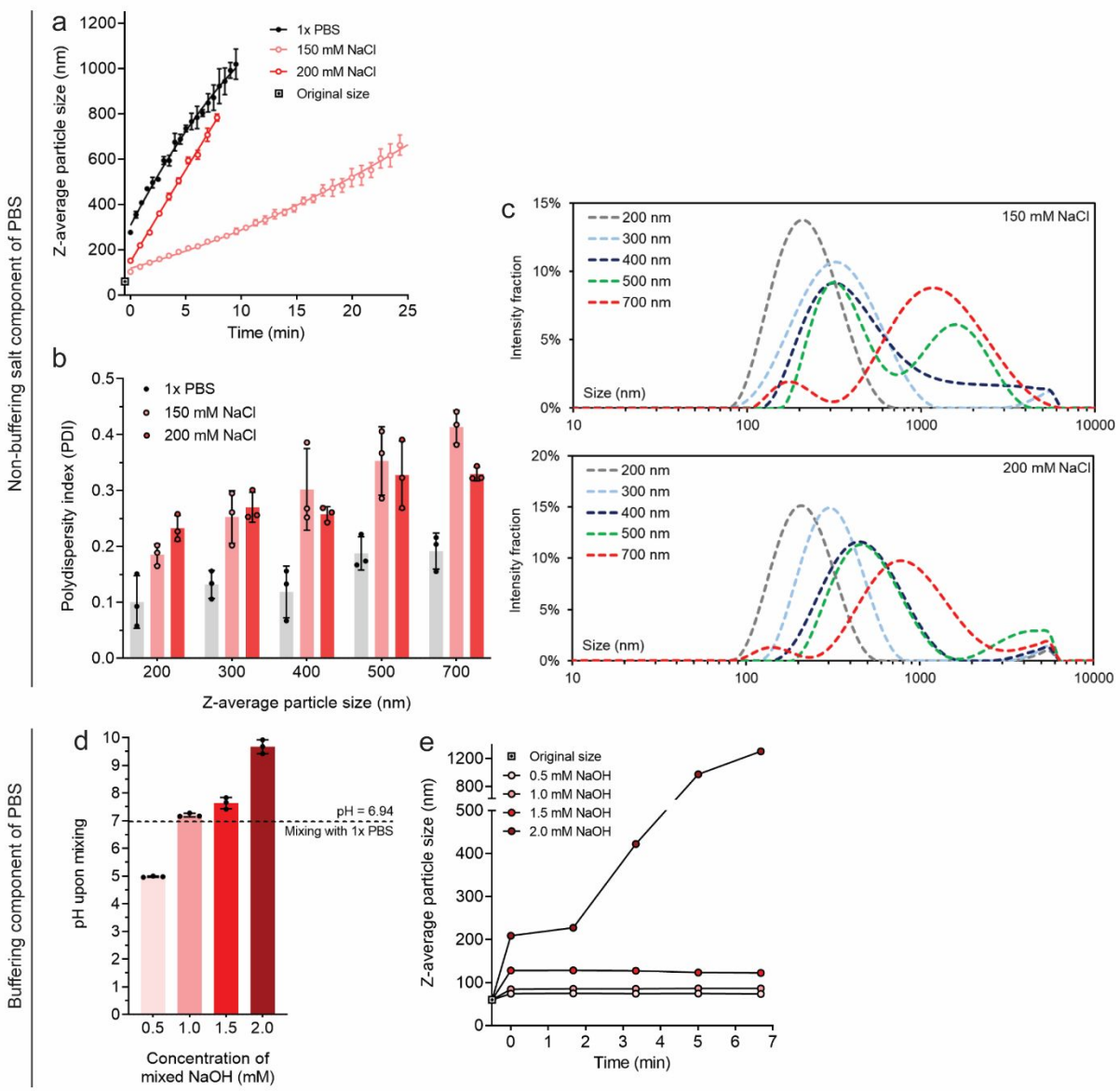

Supplementary Figure S3. Effect of ionic strength and pH of the particle growth medium on growth kinetics and uniformity. For testing the non-buffering salt component of PBS, 60-nm nanoparticles were challenged with 1× PBS-equivalent (150 mM) or elevated (200 mM) concentrations of NaCl without pH being influenced. This resulted in different **a,** size growth rates; and **b,** polydispersity index (uniformity measure provided by dynamic light scattering) or **c,** size distribution (direct uniformity illustration provided by dynamic light scattering) of particles stabilized by 20 mM HCl in 19% w/w trehalose at different sizes. For testing the buffering component of PBS, 60-nm nanoparticles were challenged with different concentrations of NaOH to mimic the pH shift. The mixing resulted in **d,** different final pH in the solution and **e,** different size growth behavior of the particles.

Additional Notes on Supplementary Figure S3: The choice of PBS as an assembly buffer.

The composition of PBS could be categorized into two subsets: pH-buffering component (namely Na_2HPO_4 and KH_2PO_4) and non-buffering salt component (namely NaCl and KCl). When using only the non-buffering salt component of a 1× PBS at the same ionic strength to induce the growth of the 60-nm nanoparticles, it showed significantly slower growth rate comparing to that of 1× PBS (**Supplementary Fig. S3a**). Using an elevated NaCl concentration of 200 mM raised the growth rate to a comparable level. However, NaCl alone could not generate uniform particles. Upon stabilization of the particles by mixing with equal volume of 20 mM HCl in 19% w/w trehalose, the polydispersity index (PDI, **Supplementary Fig. S3b** a higher uniformity correlates with a lower PDI value) and size distribution (**Supplementary Fig. S3c**) demonstrated a heterogeneous nature of the particles from a challenge by both NaCl concentrations. This was in sharp contrast to particles prepared by induction with 1× PBS, where significantly lower PDIs (**Supplementary Fig. S3b**) and distinct size peaks (main text **Fig. 2d**) were obtained. Pertaining to the size growth mechanism, insufficient deprotonation of PEI caused additional barriers for particle association. This may render the system controlled concurrently by diffusion, activation, and potentially steric effects that are a function of particle size.

Upon mixing the 60-nm nanoparticles (at a DNA concentration of 100 μg ml^{-1}) with equal volume of 1× PBS, the pH of the suspension increased from ~3 to 7. When pH was altered to ~5 to ~8 by directly mixing with NaOH solutions without involvement of non-buffering salt (**Supplementary Fig. S3d**), no size growth was observed (**Supplementary Fig. S3e**). The size of the particles did shift upwards but might be a result of shape transformation associated with gradual deprotonation of PEI in a low salt environment[3]. Only a pH shift above 9 induced a delayed, uncontrollably fast size growth. Given that the protonation fraction of PEI is still slightly higher than 40% in the pH range of 7–8, this data set indicated that partial deprotonation was not sufficient to induce particle association, and screening of the remaining charge on particle surface was vital. Thus, the non-buffering salt in PBS served as the major determinant of growing kinetics.

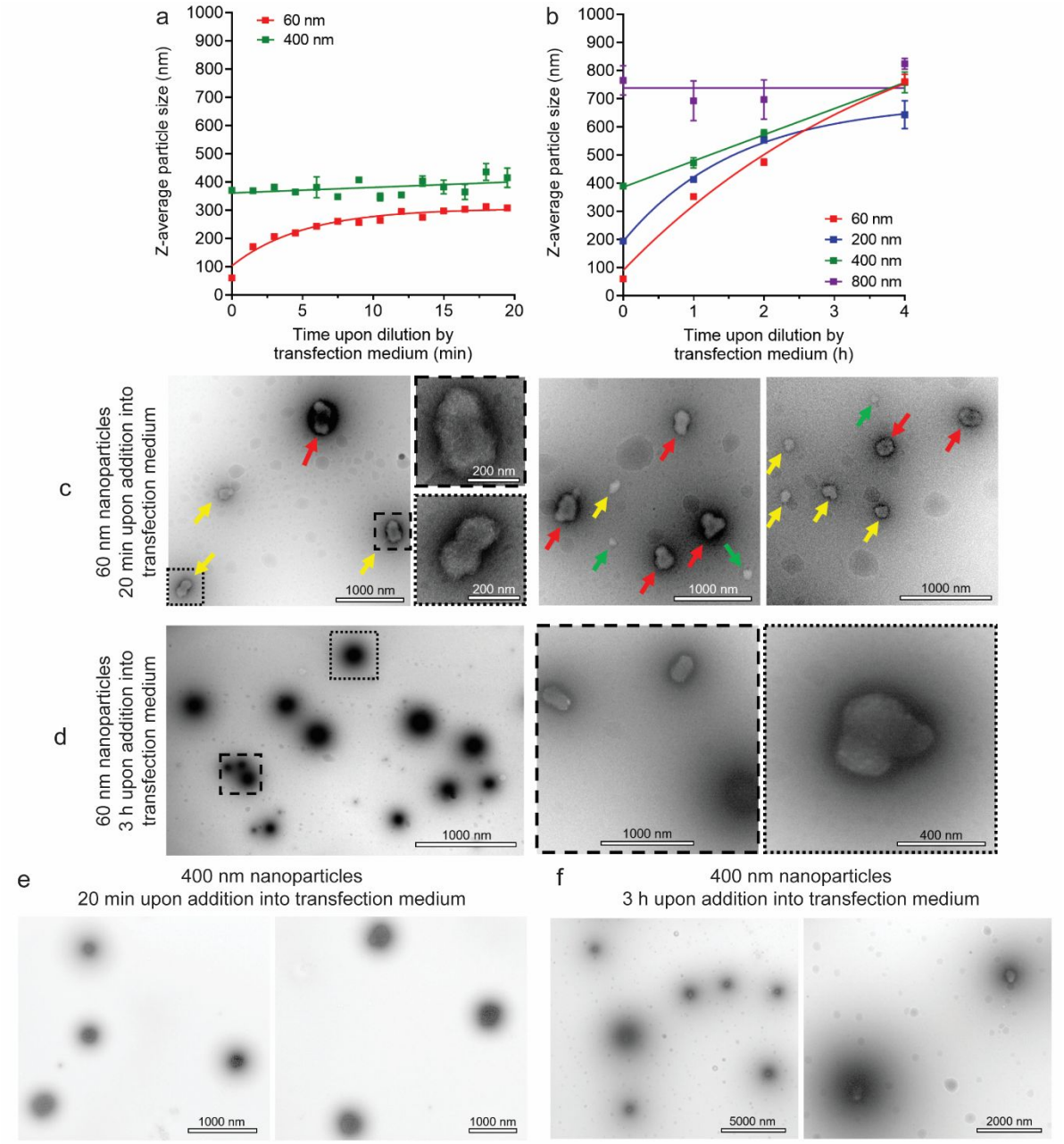

Supplementary Figure S4. The limited particle size change in transfection medium. For cell transfection experiments, the stabilized particles at a pDNA concentration of 25 μg ml^{-1} were diluted to 1 μg ml^{-1} by mixing with the transfection medium (FreeStyle 293). The size change of particles upon this dilution step was monitored by dynamic light scattering (DLS) and shown in **a,** for 60 or 400 nm particles within 20 min; and **b,** for 60, 200, 400 or 800 nm particles within 4 h. Fixation by uranyl acetate[8] with subsequent TEM observation was also used to monitor the change of particles in the diluted form in the transfection medium. Representative images are shown for 60 nm nanoparticles **c,** shortly (20 min) upon dilution or **d,** at 3 h upon dilution; and for 400 nm particles **e,** shortly (20 min) upon dilution or **f,** at 3 h upon dilution.

Additional Notes on Supplementary Figure S4:

It is without doubt that the particles could grow to larger sizes upon addition into the transfection medium (physiological salt condition, neutral pH) when they are interacting with the cells. The growth kinetics is slow due to diffusion limitation imposed by the dilution (25 folds from 25 μg pDNA ml^{-1} to 1 μg pDNA ml^{-1}), and the size growth was more profound with smaller initial size (**Supplementary Fig. S4a, b**). However, taking the 60 or 200 nm particles as examples, the significant size growth within the time scale of incubation with cells (4 h for monolayer transfection and the entire culture period, *i.e.,* 48 h for suspension transfection) still did not make them more effective (main text **Fig. 3**). This prompted us to examine if the size growth in the diluted form in transfection medium was different than the size growth by the controllable method (main text **Fig. 2**). The TEM images confirm that: (1) There was indeed a size growth for 60 nm nanoparticles. Particles with a wide range of sizes could be observed shortly upon medium dilution, with green arrows pointing to nanoparticles below 100 nm, yellow arrows pointing to particles between 100 and 250 nm, and red arrows pointing to particles above 250 nm (**Supplementary Fig. S4c**). At the same time point, DLS gave a z-average size reading of 250 nm. After 3 h, the particles grew to heterogeneously larger ones (**Supplementary Fig. S4d**) without significant differences in morphology comparing with stabilized particles in the size range of 400 nm (main text **Fig. 2F**, and **Supplementary Fig. S2d**); (2) The 400 nm particles clearly preserved the original morphology as sampled 20 min or 3 h upon dilution in transfection medium (**Supplementary Fig. S3e, f**). There was also size growth along the incubation.

In conclusion, the TEM observations confirmed the DLS monitoring results that a slow size growth did occur in the transfection medium. However, the reasons for the ineffectiveness of particles below 300 nm in size before dosing to transfection medium, even though with the ability of size growth in the medium, remain elusive. This warrants future investigations and highlights the importance of controlling the particle size **before** transfection dosage in a stable manner.

Notes on the TEM staining and imaging processing shown in Supplementary Fig. S4:

The observation of pDNA/PEI particles was enabled by negative staining using uranyl acetate. Stabilized particles with a positively charged PEI surface repel the positively charged dye, giving sharp contrast in the images showing excellent 3D structures (**Fig. 2F, Supplementary Fig. S2**). In the transfection medium, the surface charge is largely screened. Dye penetration and its interactions with pDNA were significant, rendering the particle core concentrated with the dye and too dark to observe. In such case, all images in **Supplementary Fig. S4** were applied a gamma correction with a power of 2 to 4 to make the darker areas lighter. This sacrificed the resolution and quality of the images obtained but did not affect the general discussions and conclusions.

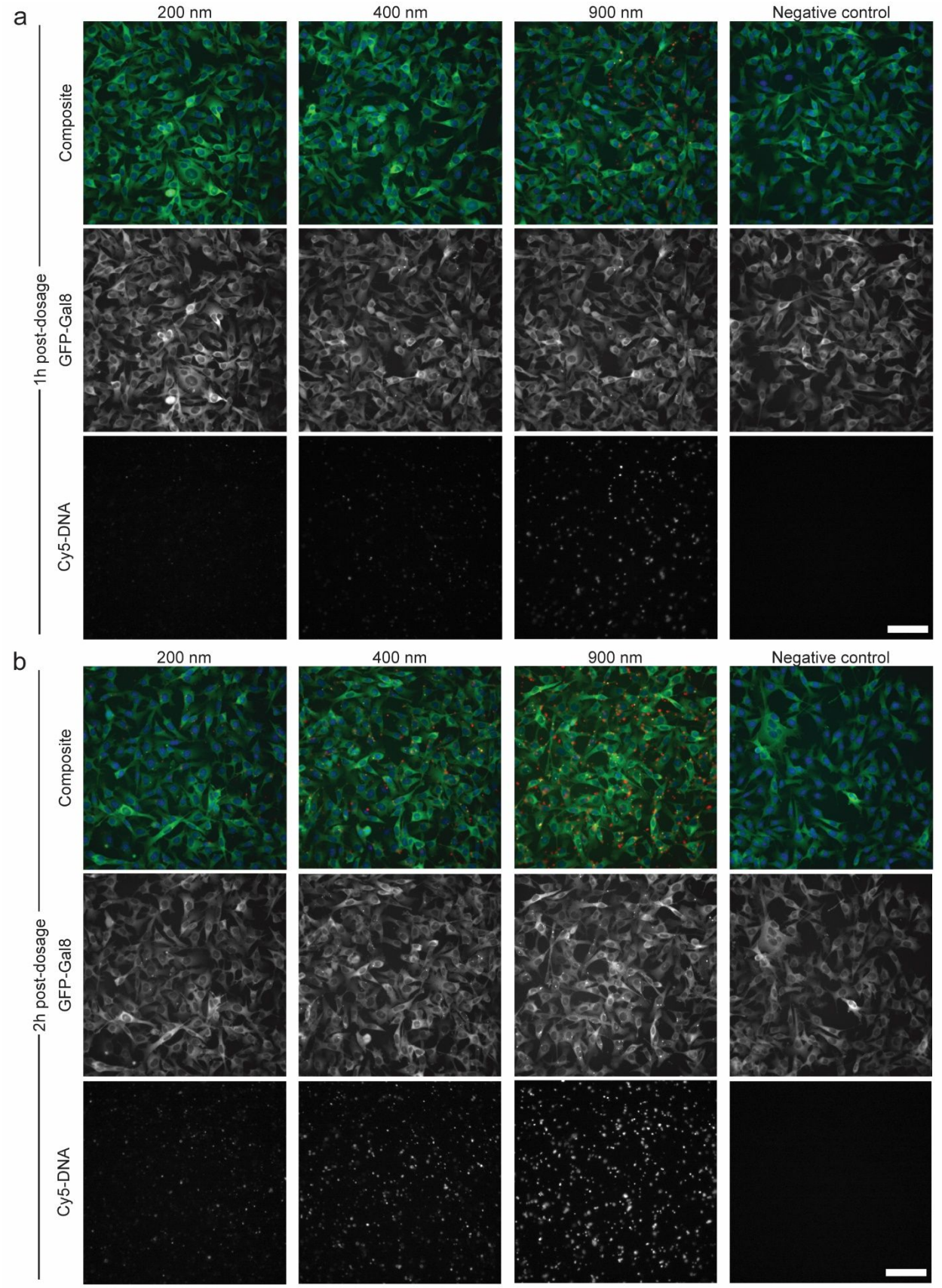
a
200 nm
400 nm
900 nm
Negative control
Composite
GFP-Gal8
Cy5-DNA
1h post-dosage
b
200 nm
400 nm
900 nm
Negative control
Composite
GFP-Gal8
Cy5-DNA
2h post-dosage

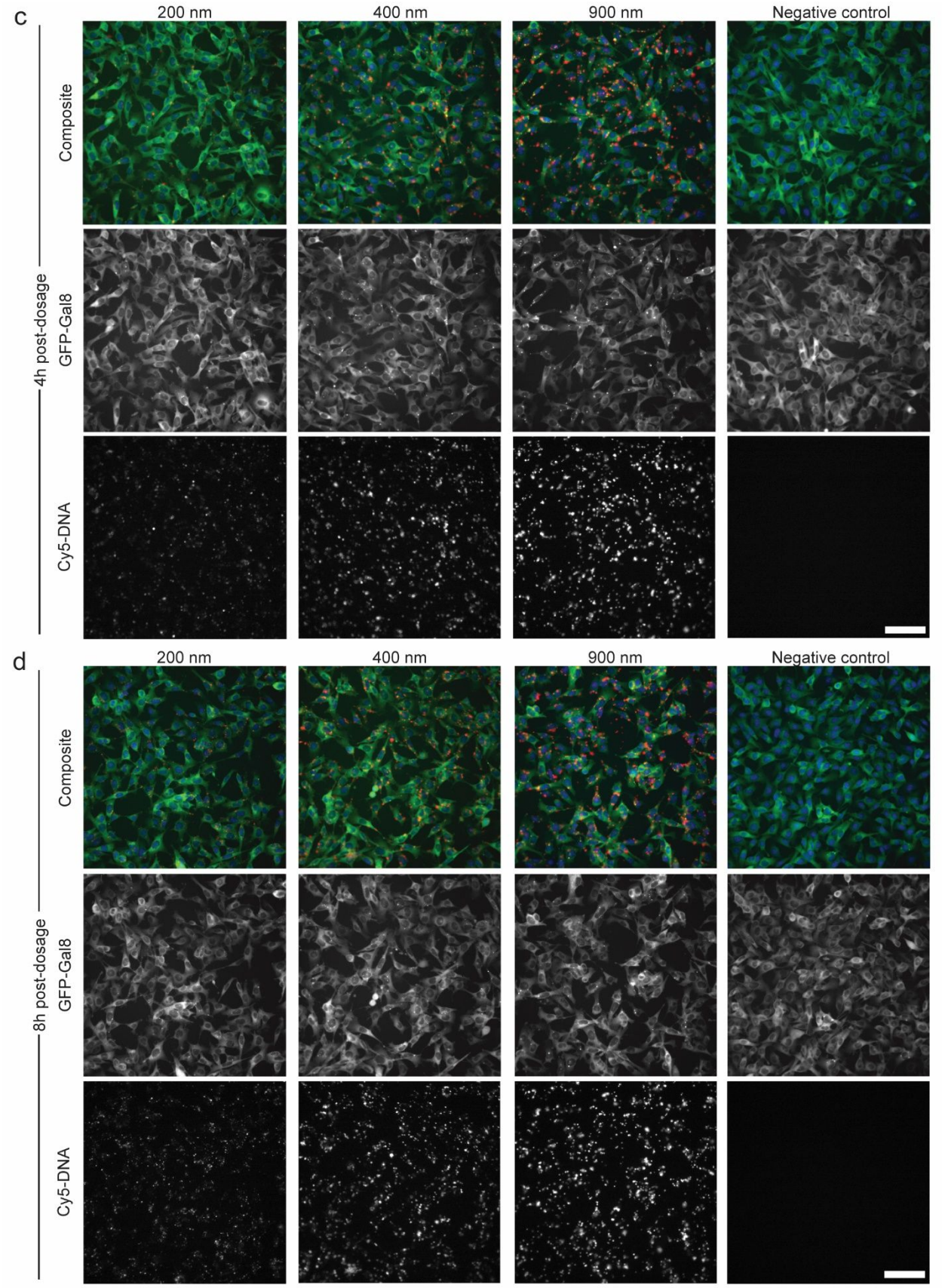
c
200 nm
400 nm
900 nm
Negative control
Composite
GFP-Gal8
Cy5-DNA
4h post-dosage
d
200 nm
400 nm
900 nm
Negative control
Composite
GFP-Gal8
Cy5-DNA
8h post-dosage

Supplementary Figure S5. Representative Cellomics images of B16F10-Gal8-GFP cells incubated with Cy5-pDNA NPs for different durations. a, 1 h; **b,** 2 h; **c,** 4 h; **d,** 8 h. Negative control: cells treated by the transfection medium (Opti-MEM) without particles for the same periods of time, for which no particle signal nor endosomal escape events (Gal8-GFP puncta) was detected. All figures share the same scale bar = 100 μm shown in the control group. These figures showed the trends seen by Cellomics quantitative analysis clearly.

Additional Notes on Supplementary Figure S5: The derivation of the 2-h and 4-h images shown in main text Fig. 4b, c.

The images shown in this supplementary figure are randomly selected from the pool of Cellomics-obtained images (1 out of 90 for each size group). To demonstrate the particle-cell interactions in greater details, a frame that is 1/4 the original area of the image was created to include a representative region, and then enlarged 4 times to generate each image in **Fig. 4b, c**.

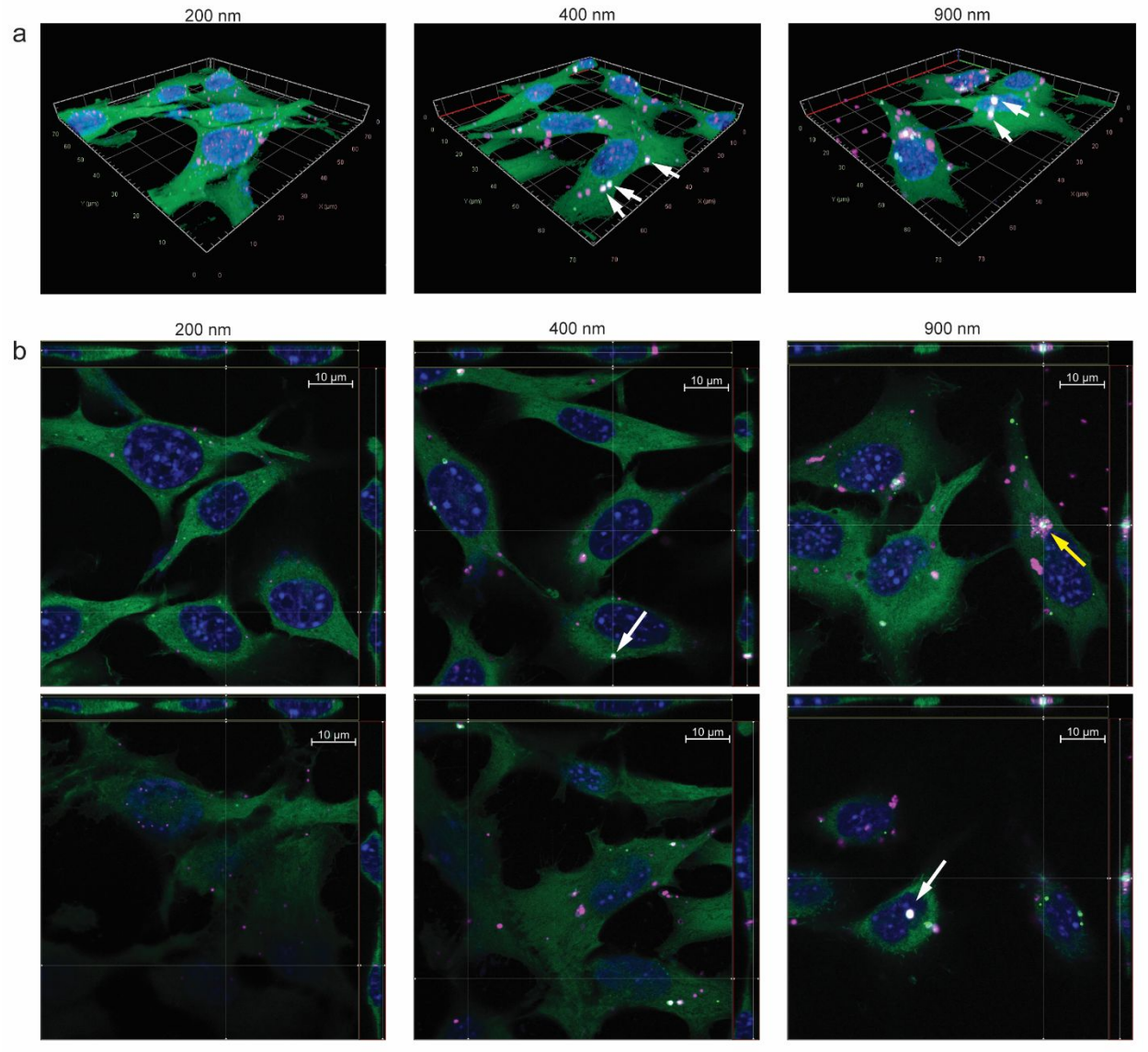

Supplementary Figure S6. Confocal laser scanning microscopy images of B16F10-Gal8-GFP cells incubated with Cy5-pDNA particles for 4 h. a, The 3D view from a z-stack experiment scanning every 0.15 μm height of the cells. **b,** Representative layer images sampled in the middle height of the cells (top panel), or at the cell base (for 200 or 400-nm groups) / the cell top (for 900-nm group). Color schemes: Hoechst 33342 (blue); GFP-Gal8 (green); Cy5-DNA (purple); colocalization of GFP and Cy5 (white).

Additional Notes on Supplementary Figure S6:

The observations by confocal laser scanning microscopy confirmed the major findings from high-throughput Cellomics measurements that: (1) Particle size differences were clearly distinguished inside the cells among different groups, and larger particles induced larger endocytic vesicles suggested by larger Gal8-GFP

puncta; (2) The level of endosomal escape scales with the overall uptake level, that a larger size inducing higher endosomal escape levels.

It is also worth noting that: (1) The white arrows show overlap of the particle signals with the endosomal escape indicator Gal8-GFP puncta. This suggests that some particles induced endosomal rupture but are still associated with the damaged vesicle membranes; (2) The yellow arrow in 900-nm group shows satellite-distributed, small particles that were seemingly dissociated from a giant one that just escaped from its endosome. The body of the giant particle is still associated with the damaged vesicle membranes; (3) For smaller particles, especially the 200-nm group, the particles concentrated near the basolateral side where the cells attach to the surface, as shown in the bottom panel for 200-nm and 400-nm groups in **Supplementary Fig. S6b**. Such feature was not observed for 900-nm group. The implications from (2) and (3) are still illusive to us and are not the focus of this study.

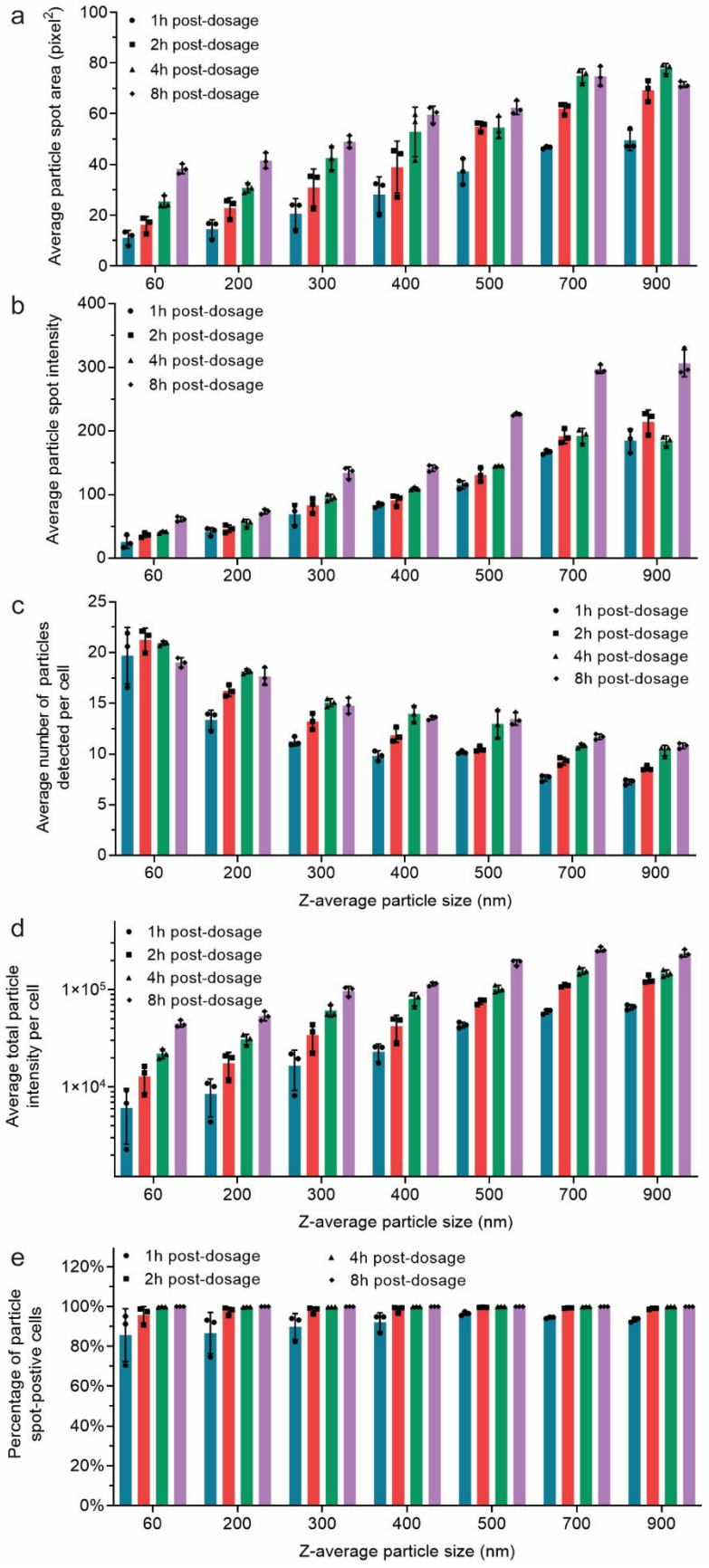

Supplementary Figure S7. Complete data set of the particle cellular uptake assessed by Cellomics. The **a,** average particle spot area; **b,** average particle spot intensity; **c,** average number of particles detected per cell; **d,** average total particle intensity per cell (the indicator of total uptake amount), and **e,** percentage of particle spot-positive cells assessed by Cellomics high-content analysis at 1, 2, 4, and 8 h post-dosage of Cy5-labeled DNA particles.

Note that: The 2-h data points in **a** and **b** are shown in main text **Fig. 4d**; The 2-h data points in **c** are shown in main text **Fig. 4f**; All the data points in **d** are shown in main text **Fig. 4g**; The 2-h data points in e are shown in main text **Fig. 4f**.

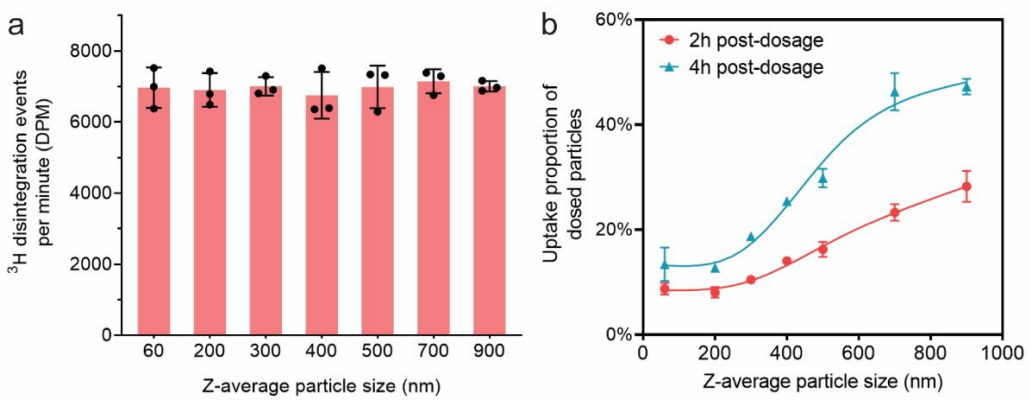

Supplementary Figure S8. Verification of the particle cellular uptake by pDNAs labeled with tritium. **a,** Disintegration events per minute (DPM) detected in control samples (100 µl of suspension of stabilized particles with 0.5 µg pDNA) for particles at different sizes, showing no influence of particle size on the scintillation assay. **b,** Absolute uptake measure of particles at different sizes after particle incubation for 2 or 4 h, relative to a total dosage of 0.1 µg pDNA per 10^4 cells.

Additional Notes on Supplementary Figure S8: ^{3}H labeling of pDNA and assessments of absolute cellular pDNA uptake.

This method was described fully in our previous reports.[2, 9] The use of this radioactive substrate tritium was approved by Johns Hopkins University Radiation Safety Office. Briefly, the pDNA was labeled by ^{3}H through methylation reaction mediated by methyltransferase (New England BioLabs, USA) with the substrate of SAM[^{3}H] (adenosyl-L-methionine, S-[methyl-^{3}H]) (PerkinElmer, USA). The pDNA was then subjected to column washing using a standard QIAprep Spin Miniprep pDNA purification kit (Qiagen, USA). The labeled pDNA was blended with unlabeled pDNA before formulation of particles and dosage to the cells as described in the main text. At 2 or 4 h post-dosage, the transfection medium containing the particles were drained, followed by intense washing of heparin-containing PBS (100 IU ml^{-1}, to remove surface-bound particles) and fresh PBS. The cells were lysed by 2 freeze-thaw cycles in reporter lysis buffer, with the lysate mixed with an equal volume of SOLVABLE solution (PerkinElmer, USA). The SOLVABLE solution solubilized ^{3}H labeled nucleotides that gained access to Ultima Gold scintillation fluid (PerkinElmer, USA) added subsequently. The radioactivity (disintegration per minute, DPM, a quantitative measure of the absolute ^{3}H amount) was assessed by a Tri-Carb 2200CA liquid scintillation analyzer (Packard Instrument Company, USA). **Supplementary Fig. S8a** demonstrated that this tritium labeling assay could accurately assess the absolute pDNA amount regardless of the particle size when particles were stabilized at different sizes and subjected to the same volume treatment of reporter lysis buffer and SOLVABLE solution. **Supplementary Fig. S8b** showed the same trend and relative relationships among groups as the semi-quantitative uptake assessment of fluorescence (average total particle intensity per cell, **Fig. 4g** in main text) by Cellomics high-content analysis. This verified the uptake behaviors of particles at different sizes.

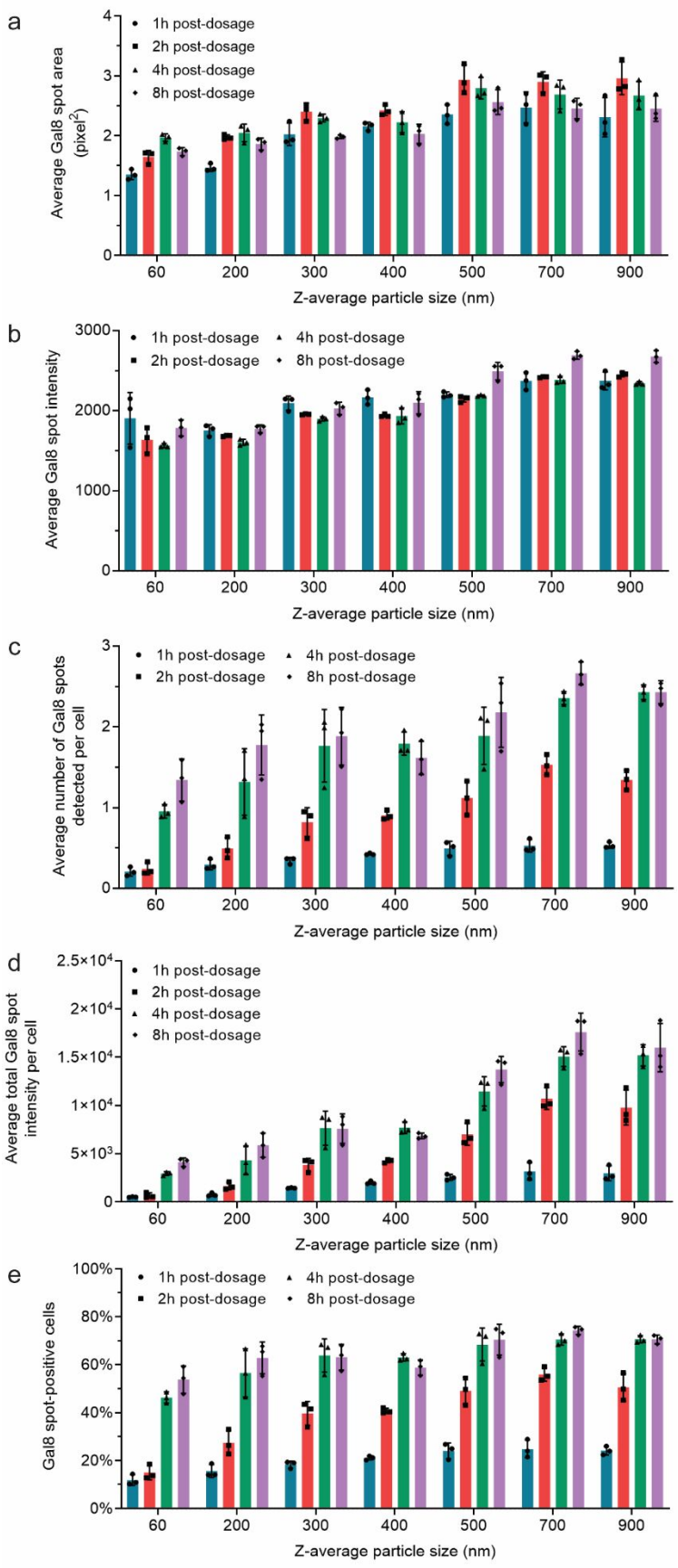

Supplementary Figure S9. Complete data set of the particle-induced endosomal escape assessed by Cellomics. The **a,** average Gal8 spot area; **b,** average Gal8 spot intensity; **c,** average number of Gal8 spots detected per cell; **d,** average total Gal8 spot intensity per cell (the indicator of total endosomal escape level); and **e,** Gal8 spot-positive cell percentage assessed by Cellomics high-content analysis at 1, 2, 4, and 8 h post-dosage of Cy5-labeled DNA particles.

Note that: The 2-h data points in **a** and **b** are shown in main text **Fig. 4e**; All the data points in **c** are shown in main text **Fig. 4h**; All the data points in **d** are shown in main text **Fig. 4i**; The 2-h data points in **e** are shown in main text **Fig. 4f**.

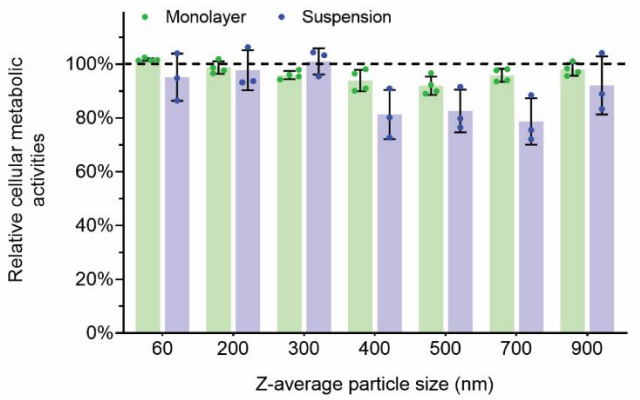

Supplementary Figure S10. Metabolism activities of cells incubated with particles at different sizes.

Additional Notes on Supplementary Figure S10:

The alamarBlue reagent (Thermo Fisher Scientific, USA) was added to HEK293T cells after they were incubated with the pDNA/PEI particles for 4 h in monolayer culture or added to HEK293F cells together with the pDNA/PEI particles. The assay reagent stayed in the medium for 20 h for monolayer culture and 48 h for suspension culture. The 100% reference level was derived from control cells treated with particle-free transfection medium. An absorbance-based assay at the wavelengths of 570 and 600 nm was conducted to 100 µl of final media following the protocol from the manufacturer.

The results showed that: (1) Even though uptake increased with larger size of the particles, there was no associated reduction in cellular metabolic activities. This suggested that the reduction in transfection efficiency seen from 400 / 500 nm to 900 nm could not be explained by potential cytotoxicity due to higher uptake levels of particles and PEI; (2) Slight reduction in metabolic activities was seen with particle sizes that induced the highest transfection efficiency: 400 and 500 nm for monolayer culture and 400, 500 and 700 nm for suspension culture. The indication of this observation is currently unknown.

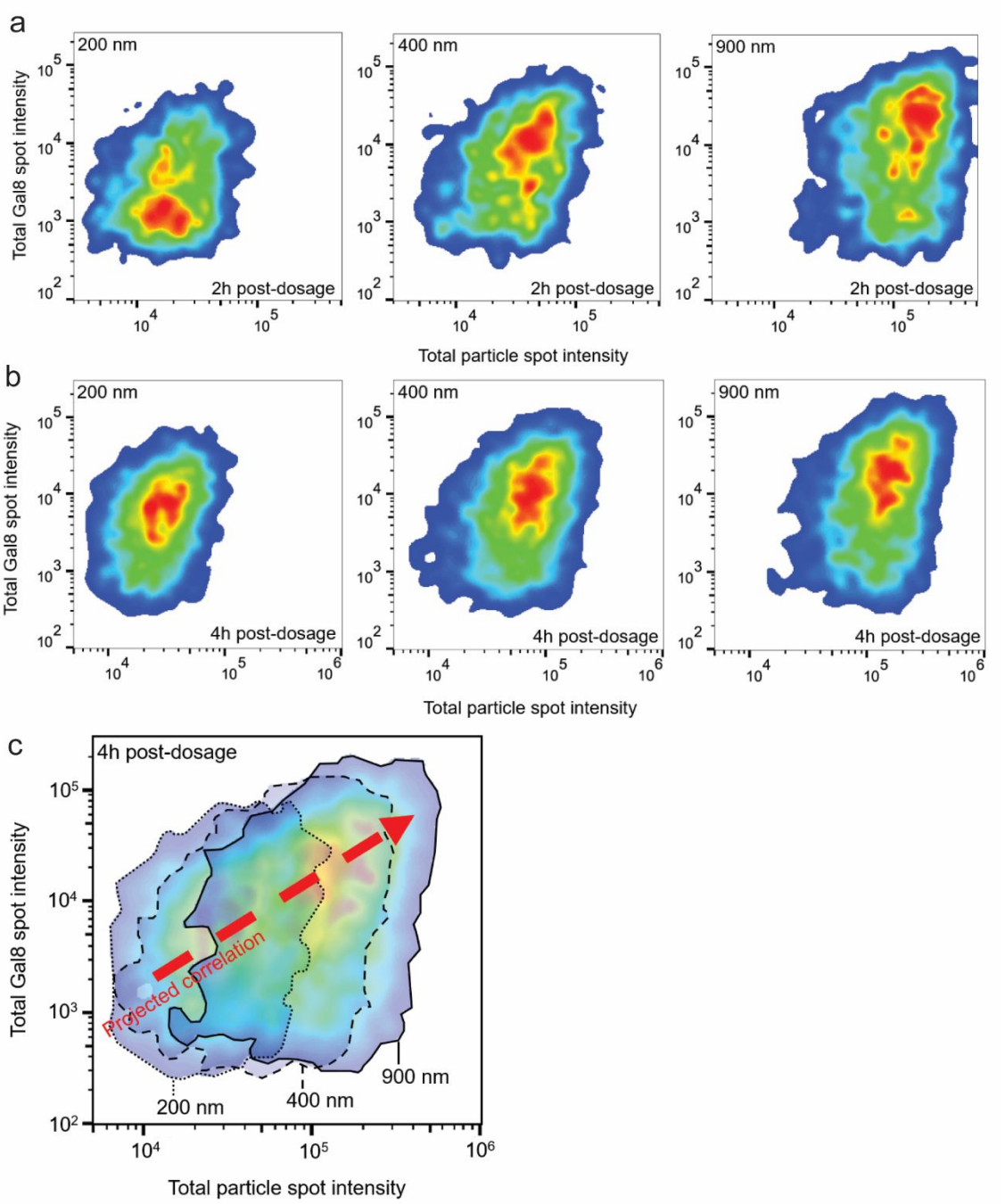

Supplementary Figure S11. Positive scaling of endosomal escape and cellular uptake on a single-cell level. The cell density heat map showing the relationship between total Gal8 spot intensity (endosomal escape level) and total particle spot intensity (cellular uptake level) on a single-cell level, for cells incubated with particles at 200, 400 or 900 nm for **a,** 2 h; and **b,** 4 h. Note that the three plots in **a** were used to generate **Fig. 4l** in the main text by overlaying with each other. Similarly, the three plots in **b** were used to generate **c**.

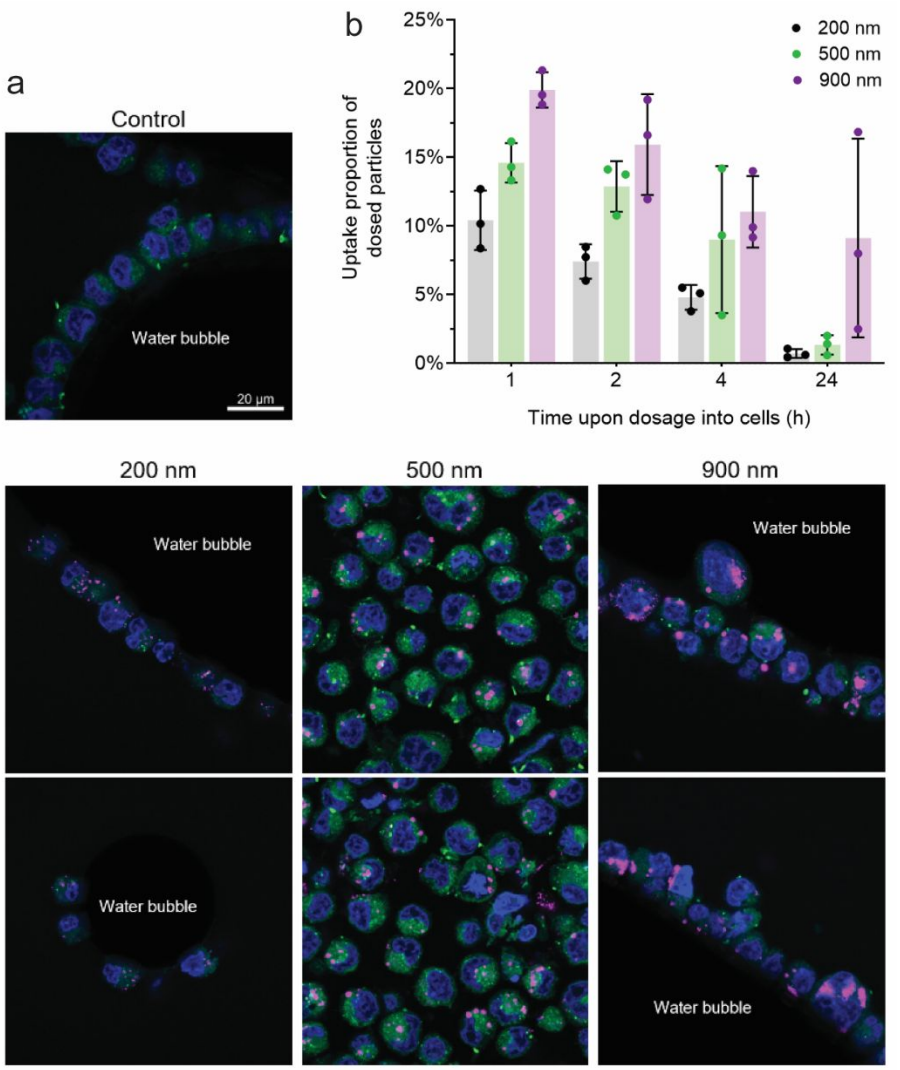

Supplementary Figure S12. Cellular uptake in suspension culture of HEK293F cells. a, Confocal laser scanning microscopy observations of cellular uptake of Cy5-pDNA particles at 2 h upon dosage. Color schemes: Hoechst 33342 (blue); CellMask Green (green). Note that this dye stained the whole cell body instead of cellular membrane, presumably due to cell membrane permeation by the fixative 4% paraformaldehyde. However it clearly marked the cell body for assessing cellular uptake; Cy5-pDNA (purple). All images share the same scale bar as that in the control image. **b,** Cellular uptake kinetics of ^{3}H-pDNA particles assessed at 1, 2, 4 and 24 h post-dosage.

Additional Notes on Supplementary Figure S12:

It is remarkable that a suspension culture of HEK293F cells showed very similar results as a monolayer culture (**Supplementary Fig. S5, S6**): (1) The particles in the cell bodies showed distinct sizes as per their relatively controlled sizes (**Supplementary Fig. S12a**), proving again that the diluted nature in the

transfection medium kinetically limited the growth of particles and preserved their size (**Supplementary Fig. S4**), and it is important to control the size before dosage; (2) The uptake positively correlated with the particle size, as qualitatively illustrated by the images and quantitatively proved by ^{3}H-labeling assay (the methods are in the associated notes under **Supplementary Fig. S8**). This assay further revealed that the intracellular pDNA quantity peaked within 1 h upon dosage and decreased as the culture continued, presenting drastic differences in uptake kinetics as a monolayer culture. This might be a result from the intense mixing conditions in the suspension culture that enabled rapid cell-particle contact shortly after dosage. Under such conditions, larger particles still exhibited greater uptake rate. These findings enhanced our view of that particle size control is the key for optimization of the transient transfection process for production of lentiviral vectors.

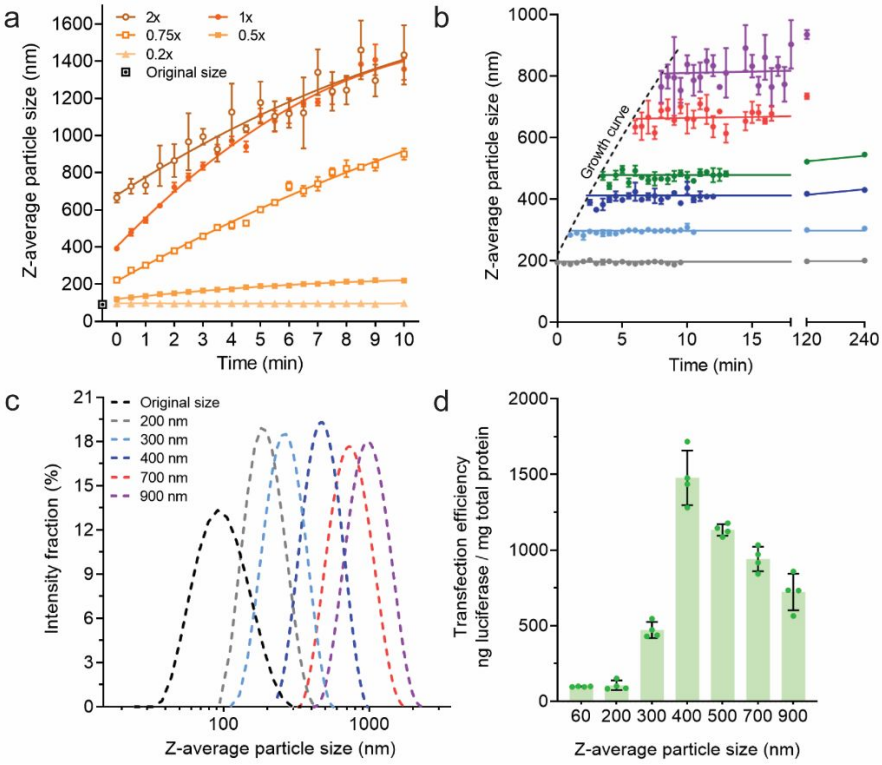

Supplementary Figure S13. Scaling the size growth process at a DNA concentration of 200 μg ml^{-1}. **a,** Predicable size growth induced under different concentrations of PBS. **b,** Particle size growth was halted by dilution with 20 mM HCl in 19% (w/w) trehalose solution at different time points along the growth curve with 0.75× PBS. **c,** The z-average diameter distributions measured by DLS of a series of stable particles with distinct sizes. **d,** The efficiency of transgene expression of luciferase as a reporter.

In these experiments, the starting DNA concentration (out of FNC preparation of the small nanoparticles) was 200 μg ml^{-1}. These small building blocks held a larger size, 80 to 100 nm, depending on the plasmid lengths. Upon solution challenge, the concentration was down to 100 μg ml^{-1} and was finally at 50 μg ml^{-1} upon particle stabilization.

SUPPLEMENTARY TABLES

Supplementary Table S1. Quality control parameters of particles prepared for bioreactor testing at bluebird bio, Inc. for LVV production (ambr® 15 micro-bioreactor scale).

Batch	**A-100**	**A-200**	**A-300**	**A-400**	**A-500**
Target size (nm)	100	200	300	400	500
Target DNA concentration (μg ml^{-1})	50	50	50	50	50
Production volumes (ml)	10	10	10	20	10
Freshly prepared samples					
Z-average diameter (nm)	107.6 ± 0.5	195.2 ± 1.9	297.6 ± 7.6	393.1 ± 14.5	519.7 ± 24.2
Polydispersity index (PDI)	0.309 ± 0.028	0.135 ± 0.020	0.176 ± 0.029	0.231 ± 0.046	0.378 ± 0.024
DNA in suspension (μg ml^{-1})	53.2 ± 0.4	49.1 ± 0.1	51.6 ± 0.5	47.5 ± 0.8	44.3 ± 2.0
Freezing to -80 °C, thawing to room temperature, immediately followed by measurements					
Z-average diameter (nm)	107.3 ± 1.9	200.7 ± 4.6	296.8 ± 5.2	404.1 ± 8.2	506.1 ± 20.1
Polydispersity index (PDI)	0.324 ± 0.005	0.106 ± 0.011	0.135 ± 0.024	0.237 ± 0.003	0.340 ± 0.103
DNA in suspension (μg ml^{-1})	52.8 ± 0.2	52.9 ± 0.4	51.7 ± 0.1	47.8 ± 0.5	42.8 ± 1.2
Freezing to -80 °C, thawing to room temperature, keeping on bench for 3 h before measurements					
Z-average diameter (nm)	111.4 ± 1.5	196.2 ± 1.6	294.7 ± 5.3	409.2 ± 12.0	509.5 ± 50.0
Polydispersity index (PDI)	0.305 ± 0.012	0.111 ± 0.010	0.181 ± 0.036	0.265 ± 0.023	0.394 ± 0.021
DNA in suspension (μg ml^{-1})	52.8 ± 0.3	51.1 ± 0.5	51.5 ± 0.8	47.3 ± 0.6	43.0 ± 1.5

Supplementary Table S2. Quality control parameters of particles prepared for bioreactor testing at bluebird bio, Inc. for LVV production (bench-scale).

Batch	**B-400-01**	**B-400-02**
Target size (nm)	400	400
Target DNA concentration (µg ml^{-1})	50	50
Production volume (ml)	100	70
Experiments	Bench-scale	Bench-scale
Freshly prepared samples		
Z-average diameter (nm)	393.3 ± 4.6	397.2 ± 3.2
Polydispersity index (PDI)	0.221 ± 0.018	0.238 ± 0.023
DNA in suspension (µg ml^{-1})	48.1 ± 0.7	49.4 ± 1.4
Freezing to -80°C, thawing to room temperature, immediately followed by measurements.		
Z-average diameter (nm)	414.9 ± 4.3	409.6 ± 0.6
Polydispersity index (PDI)	0.221 ± 0.047	0.231 ± 0.039
DNA in suspension (µg ml^{-1})	49.8 ± 0.6	50.0 ± 1.8
Freezing to -80°C, thawing to room temperature, keeping on bench for 3 h before measurements.		
Z-average diameter (nm)	405.8 ± 7.8	407.0 ± 18.7
Polydispersity index (PDI)	0.211 ± 0.021	0.247 ± 0.024
DNA in suspension (µg ml^{-1})	48.8 ± 0.7	49.9 ± 0.5

ADDITIONAL REFERENCES
for Supporting Information

1. Santos, J.L. et al. Continuous production of discrete plasmid DNA-polycation nanoparticles using flash nanocomplexation. *Small* **12**, 6214–6222 (2016).
2. Hu, Y. et al. Kinetic control in assembly of plasmid DNA/polycation complex nanoparticles. *ACS Nano* **13**, 10161–10178 (2019).
3. Johnson, B.K. & Prud'homme, R.K. Chemical processing and micromixing in confined impinging jets. *AIChE J.* 49, 2264–2282 (2003).
4. Hao, Y., Seo, J.-H., Hu, Y., Mao, H.-Q. & Mittal, R. Flow physics and mixing quality in a confined impinging jet mixer. *AIP Adv.* 10, 045105 (2020).
5. Wilson, D.R. et al. A triple-fluorophore-labeled nucleic acid pH nanosensor to investigate non-viral gene delivery. *Mol. Ther.* 25, 1697–1709 (2017).
6. Karlsson, J., Rhodes, K.R., Green, J.J. & Tzeng, S.Y. Poly(beta-amino ester)s as gene delivery vehicles: challenges and opportunities. *Expert Opin. Drug Deliv.* 17, 1395–1410 (2020).
7. Yue, Y. et al. Revisit complexation between DNA and polyethylenimine — effect of uncomplexed chains free in the solution mixture on gene transfection. *J. Control. Release* 155, 67–76 (2011).
8. Ohi, M., Li, Y., Cheng, Y. & Walz, T. Negative staining and image classification — powerful tools in modern electron microscopy. *Biol. Proced. Online* **6**, 23–34 (2004).
9. Williford, J.-M. et al. Critical length of PEG grafts on lPEI/DNA nanoparticles for efficient in vivo delivery. *ACS Biomater. Sci. Eng.* **2**, 567–578 (2016).